Chemical Structures of ZrO_2-Supported V−Sb Oxides

C. L. Pieck,[†,‡] M. A. Bañares,*[,†] M. A. Vicente,[§] and J. L. G. Fierro*[,†]

Instituto de Catálisis y Petroleoquímica, CSIC, Cantoblanco, 28049 Madrid, Spain, and Departamento de Quimica Inorgánica, Facultad de Ciencias Químicas, Universidad de Salamanca, Plaza de la Merced s/n, E-37008, Salamanca, Spain

Received April 21, 2000. Revised Manuscript Received January 22, 2001

The effect of the vanadium and/or antimony loading on the structure of zirconia and zirconium hydroxide on calcination is studied by X-ray diffraction and Raman spectroscopy. Vanadia promotes the transition of tetragonal to monoclinic zirconia at high temperatures. The interaction of dispersed vanadium oxide species with a zirconia support leads to the formation of ZrV_2O_7, which is easier on uncalcined zirconium hydroxide. Antimony tends to stabilize the tetragonal phase of zirconia and its specific area. The simultaneous presence of Sb and V on zirconia at low coverage leads to a preferential interaction of individual V and Sb oxides on the zirconia surface rather than the formation of a binary Sb−V oxide. However, at high Sb−V coverage, $SbVO_4$ is formed at the expense of surface V oxide, while the transition to monoclinic polymorph is minimized. Simultaneously, the excess of antimony forms α-Sb_2O_4.

1. Introduction

Vanadium−antimonium oxides are highly active and selective for ammoxidation reactions of several hydrocarbons such as propene, propane, and alkylaromatics.[1] The surface and bulk properties of the $VSbO_4$ phase[2,3] and mixed V−Sb oxides[4−7] have been studied in the past. However, there are current disagreements and conflicting interpretations of the structural data provided by different characterization techniques. The disagreement probably arises from the complex chemistry of the V−Sb oxides and also from the strong influence of the preparation methods on the structure of these oxides.[8] Anderson et al.[6] reported that propane activation takes place at the vanadium sites, whereas the antimonium species favor N insertion. It has been pointed out that the formal oxidation states of vanadium and antimony in the active rutile-type $VSbO_4$ structure are V^{3+} and $Sb^{5+,}$ respectively.[9,10] However, it has also been suggested that the rutile phase is a mixed oxide containing V^{3+} and V^{4+}.[4] As a general rule, the catalysts contain an excess of Sb with respect to the stoichiometry of $VSbO_4$ in order to prevent the formation of V_2O_5, which has been reported to be responsible for the oxidation of NH_3 to N_2.[6]

Additionally, it has been suggested that, during the reaction, Sb species migrate from the α-Sb_2O_4 phase toward the surface of $VSbO_4$ crystals, on which highly selective sites for the acrylonitrile formation are developed.[5] Further enhancement in the ammoxidation of propane can be obtained by adding several promoters to the V−Sb oxide systems. The highest reaction rates and selectivities were achieved by dosing with W, Te, Nb, Sn, Bi, Al, and Ti oxides.[11,12] These additives alter not only the acidity but also the redox properties of the V−Sb oxides, which play a key role in the performance.[13]

Our interest in the present work was to expand the above studies by depositing the V−Sb oxides on ZrO_2. Zirconia was used as a support because it is stable under oxidizing and reductive environments and because it has both acidic and basic surface sites. The structure of vanadium oxide on ZrO_2 is known with certain detail. Based on the Raman spectra of hydrated V/ZrO_2 samples, Deo and Wachs[14] found meta-, pyro-, and decavanadate (octahedral-type) structures, which are completely transformed into tetrahedrally coordinated V species upon dehydration. It was also observed that the V oxide deposited on ZrO_2 not only retards the sintering of ZrO_2 but also inhibits the transformation of amorphous ZrO_2 into its tetragonal phase.[15] Recently, Khodakov et al.[16]

* Corresponding authors. E-mails: jlgfierro@icp.csic.es, mbanares@icp.csic.es.

† CSIC.

‡ On leave from INCAPE (FIQ-UNL, CONICET), Santiago del Estero 2654, 3000 Santa Fe, Argentina.

§ Universidad de Salamanca.

(1) See, e.g.: Moro-oka, Y.; Ueda, W. In *Catalysis*; Royal Chemical Society: Cambridge, U.K., 1994; Vol. 11, p 223.

(2) Berry, F. J.; Brett, M. E.; Patterson, W. R. *J. Chem. Soc., Dalton Trans.* **1983**, 9.

(3) Berry, F. J.; Brett, M. E.; Holden, J. G.; Labarta, A.; Rodriguez, R.; Tejada, J. *Inorg. Chim. Acta* **1985**, *105*, 197.

(4) Centi, G.; Foresti, E.; Guarnieri, F. *Stud. Surf. Sci. Catal.* **1994**, *82*, 281.

(5) Nilsson, R.; Lindblad, T.; Andersson, A.; Song, C.; Hansen, S. *Stud. Surf. Sci. Catal.* **1994**, *82*, 293.

(6) Andersson, A.; Andersson, S. L. T.; Centi, G.; Grasselli, R. K.; Sanati, M.; Trifiro, F. *Appl. Catal. A: Gen.* **1994**, *113*, 43.

(7) Landa-Canovas, A.; Nilsson, J.; Hansen, S.; Stahl, K.; Andersson, A. *J. Solid State Chem.* **1995**, *116*, 369.

(8) Centi, G.; Mazzoli, P.; Perathoner, S. *Appl. Catal. A: Gen.* **1997**, *165*, 273.

(9) Berry, F. J.; Brett, M. E. *J. Catal.* **1984**, *88*, 232.

(10) Birchall, T.; Sleight, A. W. *Inorg. Chem.* **1976**, *15*, 868.

(11) Guttman, A. T.; Grasselli, R. K.; Brazdil, J. F.; Suresh, D. D. U.S. Patent 4,797,381, 1989.

(12) Guttman, A. T.; Grasselli, R. K.; Brazdil, J. F.; Suresh, D. D. U.S. Patent 4,788,317, 1988.

(13) Zanthoff, H. W.; Schaefer, S.; Wolf, G. U. *Appl. Catal. A: Gen.* **1997**, *164*, 105.

(14) Deo, G.; Wachs, I. E. *J. Phys. Chem.* **1991**, *95*, 5889.

10.1021/cm000333v CCC: $20.00 © 2001 American Chemical Society
Published on Web 03/16/2001

confirmed that vanadium oxide dispersed on a $ZrO(OH)_2$ (330 m^2/g) retards the crystallization of ZrO_2 during calcination as well as the tetragonal-to-monoclinic phase transformation. Apart from these studies, very little is known about the structure of Sb oxides deposited on ZrO_2 and its influence on the ZrO_2 phase transformation, and even less is known about the influence of Sb oxide on the structure of vanadium oxide when both are incorporated on the ZrO_2 surface. Accordingly, our aim was to characterize the structure of vanadium and antimony oxides deposited on a high-specific-area ZrO_2 substrate and how their loadings influence their structures upon calcination.

2. Experimental Section

2.1. Preparation of the Supported Oxides. A 3.5% silica-stabilized $Zr(OH)_4$ precursor was provided by MEL Chemicals (1.7% HfO_2). Two series of zirconia-supported oxides were prepared. The first was prepared from $Zr(OH)_4$ previously calcined in air at 923 K for 4 h, and the second from the $Zr(OH)_4$ precursor without calcination. The materials prepared from the precalcined Zr precursor will be referred to as V/ZrO_2, $Sb-V/ZrO_2$, or Sb/ZrO_2, whereas those prepared from the noncalcined $Zr(OH)_4$ precursor are labeled V/ZrOH, Sb−V/ZrOH, or Sb/ZrOH. Loadings on both series are indicated by the total number of atoms (V + Sb) supported per square nanometer of support. The V/ZrO_2 and V/ZrOH materials were prepared by impregnation in excess of solution. The [$Zr(OH)_4$ or ZrO_2] support was immersed in a solution of HNO_3 in deionized water at pH = 2, and then a precise amount of NH_4VO_3 was added. The excess of water was removed in a rotary evaporator at 353 K. Then, the precursors were dried in air in an oven at 393 K for 16 h and, finally, were calcined in air at 923 K for 4 h. Four different samples, containing 1.6, 4.0, 8.0, and 16.0 atoms of V and/or Sb per nm^2 of support (calculated on the basis of a specific area of 86 m^2/g of the calcined support), were prepared. It has been reported that the dispersion limit on zirconia is close 8 V atoms per nm^2, which should correspond to a monolayer.[17] For the Sb/ZrO_2 and Sb/ZrOH series, the Sb_2O_3 was kept in solution according to the procedure developed in our laboratory,[18] and hence, the preparation was the same as for the V/ZrO_2 series. Samples containing 1.6 and 8.0 Sb atoms/nm^2 were prepared. The ternary $Sb-V/ZrO_2$ and Sb−V/ZrOH systems, containing both V and Sb, were prepared by impregnating the support with aqueous solutions of the two oxides. The series were prepared with 1.6, 8.0, and 16.0 Sb−V atoms/nm^2 and a fixed atomic ratio (Sb/V = 3).

Bulk $SbVO_4$ samples were prepared by mixing aqueous solutions of NH_4VO_3 and Sb_2O_3 of appropriate concentrations to yield atomic ratios of Sb/V = 1 and 3. The drying and calcination steps were the same as above. A reference ZrV_2O_7 compound was prepared by adding the stoichiometric amount of $Zr(OH)_4$ to a solution of NH_4VO_3 to obtain an atomic ratio of V/Zr = 2. Excess water was removed in a rotary evaporator at 353 K. Then, the dried precursor was kept in an oven at 393 K for 16 h and subsequently calcined at 973 K for 24 h.

2.2. Experimental Techniques. Nitrogen adsorption isotherms (77 K) were recorded on an automatic Micromeritics ASAP-2000 apparatus. Prior to the adsorption experiments, samples were outgassed at 413 K for 2 h. BET areas were computed from the adsorption isotherms (0.05 < P/Po < 0.27), taking a value of 0.164 nm^2 for the cross section of the adsorbed N_2 molecule at 77 K.

Table 1. BET Areas of Catalysts Calcined in Air at 923 K for 4 h

	BET area (m^2/g)	
Sb + V atoms/nm^2	ZrO_2 support	ZrOH support
0	86	−
1.6 V	62	71
4.0 V	19	9
8.0 V	10	5
16.0 V	7	5
1.6 Sb	73	65
4.0 Sb	62	15
1.6 Sb−V	69	44
8.0 Sb−V	52	50
16.0 Sb−V	28	35
$SbVO_4$ (Sb/V = 1) (bulk)	6	
$SbVO_4$ (Sb/V = 3) (bulk)	5.5	
ZrV_2O_7 (bulk)	<1	

X-ray diffraction patterns were recorded on a Siemens Krystalloflex D-500 diffractometer using Cu Kα radiation (λ = 0.15418 nm) and a graphite monochromator. Working conditions were 40 kV, 30 mA, and scanning rate of 2°/min for Bragg's angles (2θ) from 5° to 70°.

Raman spectra were run with a single-monochromator Renishaw System 1000 spectrometer equipped with a cooled CCD detector (200 K) and a holographic super-Notch filter. The latter filters the elastic scattering, so that the Raman signal remains higher than when triple-monochromator spectrometers are used. The samples were excited with the 514-nm Ar line; the spectral resolution was ca. 3 cm^{-1}, and spectrum acquisition consisted of 10 accumulations of 30 s. The spectra were obtained under dehydrated conditions (ca. 390 K) in a hot stage (Linkam TS-1500). Hydrated samples were then obtained at room temperature under exposure to a stream of humid synthetic air. In situ Temperature-Programmed Raman (TP-Raman) experiments were conducted under flowing synthetic air (SEO, L'Air Liquide) with a hot stage (Linkam TS-1500**)** attached to the micro-Raman system. TP-Raman experiments were performed by heating samples from 323 to 973 K in steps of 50 K. Spectra were acquired by 10 accumulations of 30 s at each temperature.

3. Results

Table 1 summarizes the specific areas of the oxides calcined in air at 923 K for 4 h. The BET area depends on the metal oxide loading. For the V-loaded oxides, the specific areas decreased with vanadium loading, much more so at high V contents. For the Sb- and Sb−V-loaded series, the same decay was observed, although it was less marked than for the V counterparts.

Figure 1 shows the XRD patterns of the V/ZrOH series, together with those of the V-free support calcined at 923 K and the reference ZrV_2O_7 compound. The V-free support displays a diffraction peak at 30.5°, presumably due to the presence of the tetragonal (or cubic) phase. However, the absence of diffraction peaks at 28.2° and 31.5° precludes the presence of the monoclinic phase.[19] Incorporation of a small amount of V (1.6 V atoms/nm^2) induces ZrO_2 phase transformation. At 4.0 V atoms/nm^2 and above, 100% of the monoclinic phase was reached, and simultaneously, diffraction peaks at 16°, 20°, 22.5°, and 24.8°, characteristic of the ZrV_2O_7 phase, are observed.[20] The V/ZrO_2 series showed the same behavior (for the sake of simplicity, the

(15) Sohn, J. R.; Cho, S. G.; Pae, Y. I.; Hayashi, S. *J. Catal.* **1996**, *159*, 170.
(16) Khodakov, A.; Yang, J.; Su, S. C.; Iglesia, E.; Bell, A. T. *J. Catal.* **1998**, *171*, 343.
(17) Wachs, I. E. *Catal. Today* **1996**, *27*, 437.
(18) Guerrero-Pérez, O. et al., manuscript in preparation.
(19) *Selected Power Diffraction Data For Metals and Alloys. Data Book*, 1st ed.; International Center for Diffraction Data (JCPDS): Swarthmore, PA; Vol II, Cards 13-307 and 24-1164.

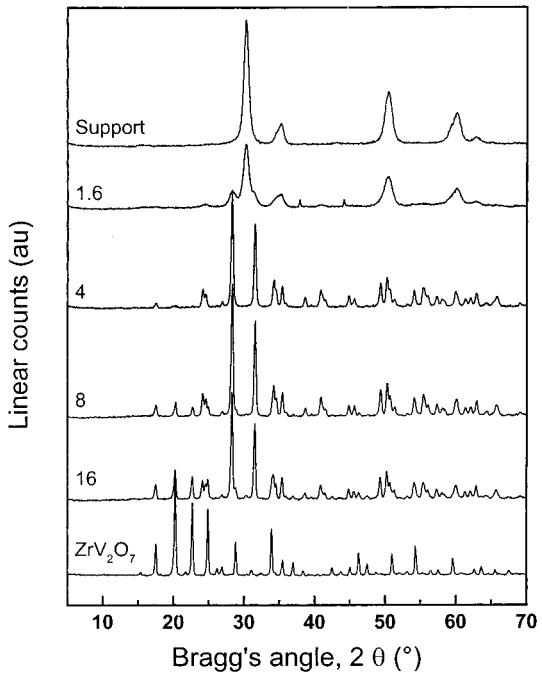

Figure 1. XRD patterns of the V/ZrOH series, of the support after calcination at 923 K, and of the ZrV_2O_7 reference compound.

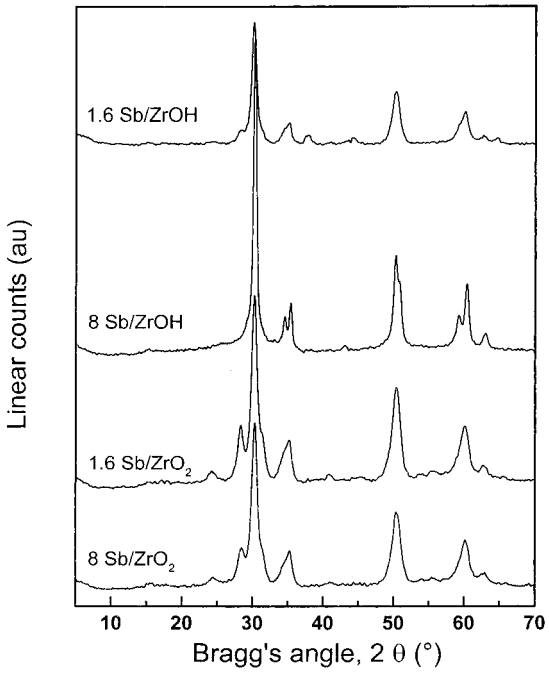

Figure 2. XRD patterns of Sb/ZrO_2 and Sb/ZrOH.

diffractograms are not included). However, complete transformation of the tetragonal to the monoclinic phase required higher V-loading values (8.0 V atoms/nm^2) than for the V/ZrOH series. Figure 2 shows the XRD patterns of the Sb/ZrO_2 and Sb/ZrOH series. It is clear that the zirconia phase remains for 1.6 and 8.0 Sb atoms/nm^2. The tetragonal phase predominates, although the monoclinic structure is incipient in the Sb/ZrOH series (reflection at 28.2° and shoulder at 31.5°),[21] and becomes evident in the Sb/ZrO_2 series.

(20) *Selected Powder Diffraction Data For Metals and Alloys. Data Book*, 1st ed.; International Center for Diffraction Data (JCPDS): Swarthmore, PA; Card 16-0422.

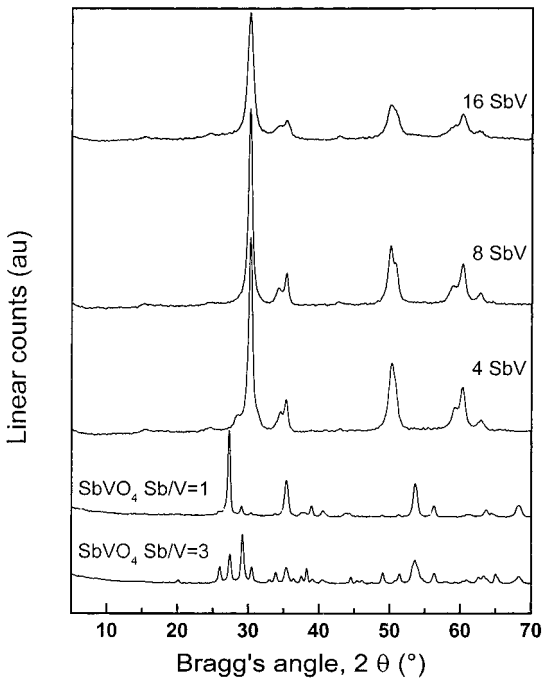

Figure 3. XRD patterns of Sb−V/ZrOH and of bulk $SbVO_4$.

The V−Sb-containing zirconia samples display a tetragonal structure at high V−Sb loading, with only a minor amount of the monoclinic phase for 4.0 V−Sb/ZrOH (Figure 3). Moreover, no diffraction lines of ZrV_2O_7 are observed. In the $Sb-V/ZrO_2$ series, both tetragonal and monoclinic phases coexist at low Sb−V loading, although the tetragonal phase predominates. However, only the tetragonal phase is developed at higher Sb−V contents. The diffraction profile of the bulk $SbVO_4$ (Sb/V = 1 atom ratio) coincides with that reported for the rutile-type phase of antimony vanadate.[8,10,22] However, for the bulk sample prepared with Sb/V = 3, the $SbVO_4$ phase is accompanied by Sb_2O_4 and Sb_2O_4 cervantite (diffraction angles at 25.8 and 29°).[23] The stabilizing effect of the tetragonal phase of ZrO_2 for high Sb−V contents suggests the existence of some interaction between the two oxides, although no zirconia with Sb and V generates the diffraction pattern of the $SbVO_4$ phase. Therefore, if $SbVO_4$ is formed in these samples, it must be distributed in very small domains that cannot be detected by X-ray diffraction.

With a view toward corroborating the importance of the method of preparation on the crystal structure of zirconia, the support calcined at 923 K was pretreated with an aqueous solution of HNO_3 (pH = 2) after which the materials were prepared following the same procedure as for the V or Sb series. The ZrO_2 samples calcined at 923 K exhibited a tetragonal structure and a BET area similar to those of the calcined ZrO_2. Consequently, the preparation method has no effect on the zirconia support.

(21) *Selected Powder Diffraction Data For Metals and Alloys. Data Book*, 1st ed.; International Center for Diffraction Data (JCPDS): Swarthmore, PA; Card 74-1725.

(22) Hansen, S.; Ståhl, K.; Nilsson, R.; Andersson, A. *J. Solid State Chem.* **1993**, *102*, 340.

(23) *Selected Powder Diffraction Data For Metals and Alloys. Data Book*, 1st ed.; International Center for Diffraction Data (JCPDS): Swarthmore, PA; Card 32-0042.

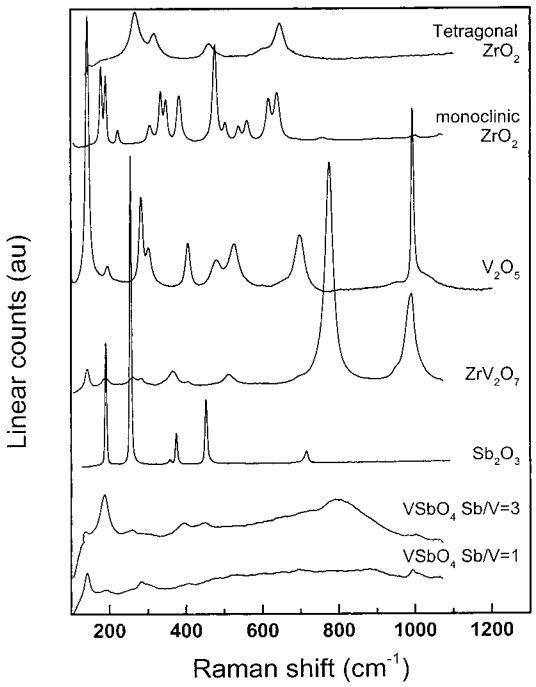

Figure 4. Raman spectra of reference compounds, bulk $SbVO_4$ with Sb/V ratios of 3 and 1, tetragonal and monoclinic ZrO_2, bulk ZrV_2O_7, crystalline V_2O_5, and bulk Sb_2O_3.

Figure 4 shows the Raman spectra of several reference compounds. The ZrO_2 monoclinic phase shows bands at 178, 187, 223, 307, 335, 383, 477, 538, 560, 617, and 639 cm^{-1},[24] whereas for the ZrO_2 tetragonal phase, the bands appear at 143, 263, 325, 474, 608, and 640 cm^{-1}. The Raman bands of crystalline V_2O_5 appear at 147, 190, 694, and 994 cm^{-1}, and those of ZrV_2O_7 appear at 780 and 990 cm^{-1}, in agreement with previous results[25−27] (the band at 143 cm^{-1} corresponds to a small excess of unreacted V_2O_5). For Sb_2O_3, the bands are located at 190, 259, 374, 455, and 715 cm^{-1}. Finally, the bulk $SbVO_4$ (Sb/V = 3) oxide displays bands at 190 and 397 cm^{-1}, associated with α-Sb_2O_4,[28] and a broad peak from 750 to 950 cm^{-1}, presumably due to the rutile-type phase of $SbVO_4$. However, $SbVO_4$ (Sb/V = 1) shows peaks at 143, 283, 523, 694, and 994 cm^{-1}, which are ascribed to V_2O_5.

Figure 5 shows the Raman spectra of the calcined ZrO_2 support and of the V/ZrOH and V/ZrO_2 series. The support is 100% tetragonal, as indicated by the Raman bands at only 263, 325, 472, 608, and 640 cm^{-1}. At low vanadia coverages, a transition to the monoclinic phase is evident (new modes near 175, 190, and 477 cm^{-1}). This phase transition also takes place for the V/ZrO_2 series, in which the support had previously been calcined at 923 K (Figure 5). The Raman band close to 143 cm^{-1} at 1.6 V atoms/nm^2 does not correspond to crystalline V_2O_5, but rather to the tetragonal ZrO_2 phase,

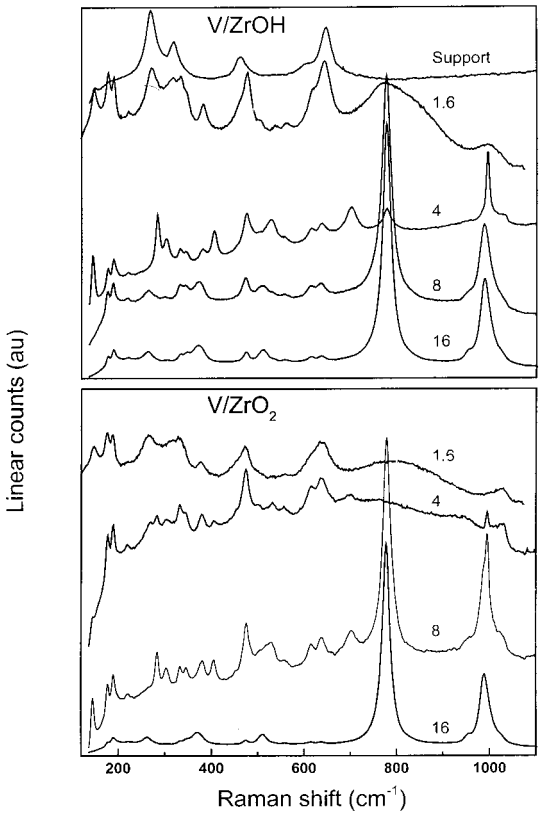

Figure 5. In situ Raman spectra of dehydrated V/ZrO_2, V/ZrOH, and the ZrO_2 support.

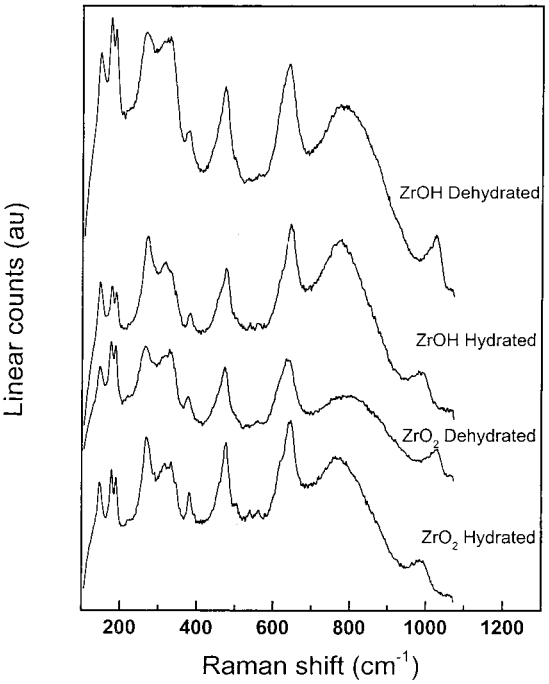

Figure 6. In situ Raman spectra of hydrated and dehydrated 1.6 V/ZrO_2 and 1.6 V/ZrOH.

because no other bands of crystalline V_2O_5 are present, but there is a band at 1030 cm^{-1}, which must correspond to surface-dispersed vanadium oxide species. Figure 6 shows the in situ Raman spectra of 1.6 V/ZrO_2 and 1.6 V/ZrOH under dehydrated and hydrated conditions. The band at 1030 cm^{-1} is sensitive to hydration, which confirms that it belongs to the dispersed vanadium oxide species as crystals are not sensitive to hydration treat-

(24) Miciukiewicz, J.; Mang, T.; Knözinger, H. *Appl. Catal. A: Gen.* **1995**, *122*, 151.
(25) Khodakov, A.; Olthof, B.; Bell, A. T.; Iglesia, E. *J. Catal.* **1999**, *181*, 205.
(26) Roozeboom, F.; Mittelmeijer-Hazeleger, M. C.; Moulijn, J. A.; Medema, J.; de Beer, V. H. J.; Gellings, P. J. *J. Phys. Chem.* **1980**, *84*, 2783.
(27) Sanati, M.; Andersson, A.; Wallemberg, I. R.; Rebenstorf, B. *Appl. Catal. A* **1993**, *106*, 51.
(28) Nilsson, R.; Lindblad, T.; Andersson, A. *J. Catal.* **1994**, *148*, 501.

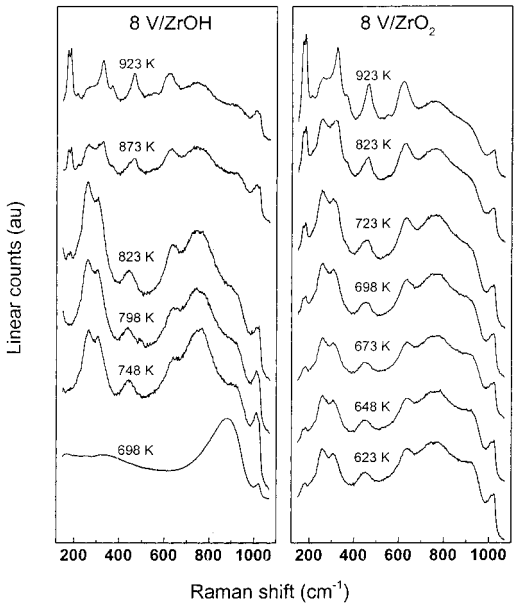

Figure 7. Representative TP-Raman spectra of the precursors of 8 V/ZrO_2 and 8 V/ZrOH under flowing dry air.

ments.[17] When the vanadium content is increased up to 4.0 V atoms/nm^2, the bands of the ZrO_2 tetragonal phase, disappear whereas those of the monoclinic phase predominate, together with new broad bands at 143, 283, 302, 405, 526, 698, and 994 cm^{-1}that are characteristic of V_2O_5. For the 4 V/ZrOH sample, broad bands at 780 and 990 cm^{-1}, characteristic of ZrV_2O_7, are distinguished. These bands are clearly differentiated at 8.0 V atoms/nm^2 and dominate the spectrum at 16.0 V atoms/nm^2.

Figure 7 shows representative TP-Raman spectra of the 8 V/ZrOH and 8 V/ZrO_2 precursors as a function of the calcination temperature. The 8 V/ZrOH precursor exhibits the monoclinic phase (bands at 175 and 190 cm^{-1}) at calcination temperatures ranging from 798 to 823 K, whereas both the monoclinic and tetragonal phases coexist on the 8 V/ZrO_2 precursor within a wide temperature range. At temperatures above 698 K, the bands of the monoclinic phase become slightly more intense. Moreover, characteristic bands of the ZrO_2 tetragonal phase (263 cm^{-1}) are found for the 8 V/ZrOH precursor at 748 K, whereas those of the monoclinic phase are seen at higher temperatures. Thus, it appears that the tetragonal phase is formed at lower temperatures and that it undergoes further transformation to the monoclinic phase at higher temperatures. This tendency was already observed upon calcination of all of the V/ZrOH precursors.

Figure 8 shows the in situ Raman spectra of the dehydrated Sb/ZrOH and Sb/ZrO_2 samples. In no case are any bands of Sb detected. Both the monoclinic and tetragonal phases of ZrO_2 are found in both series, although the bands of the monoclinic phase are much more intense in the Sb/ZrO_2 series, in agreement with the XRD profiles.

The supported Sb−V series maintain the tetragonal structure at high loading values, although the monoclinic phase is observed for low Sb−V contents (Figure 9). The broad band at 750−950 cm^{-1}, together with the band at 452 cm^{-1}, can be ascribed to the appearance of the $SbVO_4$ phase.[5] Thus, at low coverage, the V−Sb/

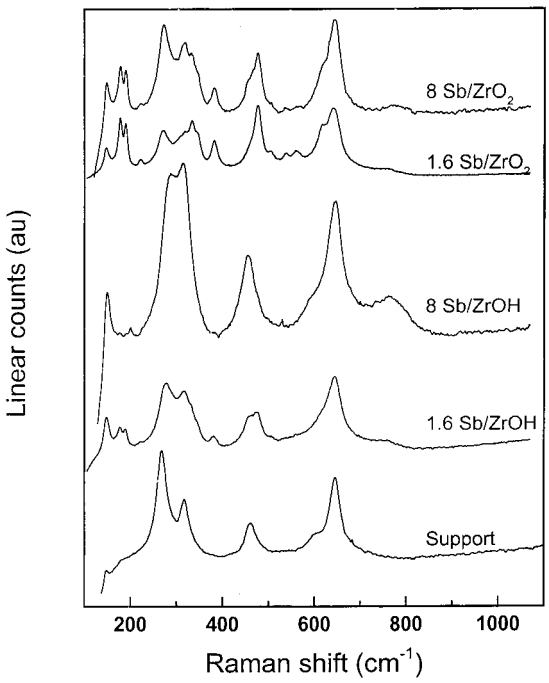

Figure 8. In situ Raman spectra of dehydrated Sb/ZrO_2, Sb/ZrOH, and the ZrO_2 support.

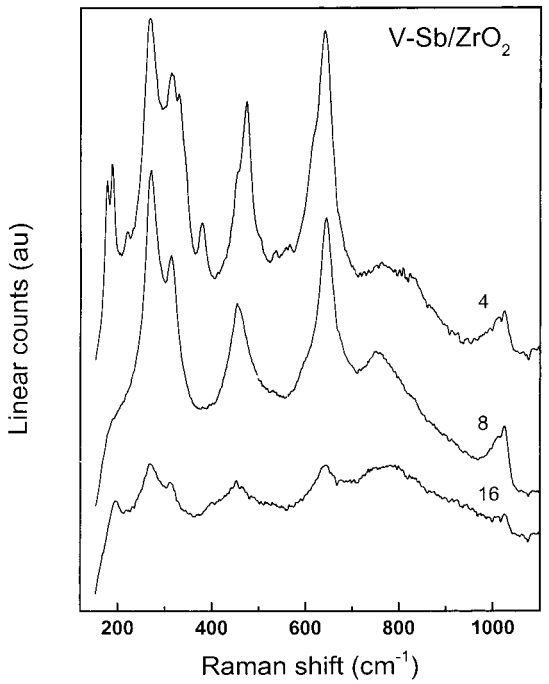

Figure 9. In situ Raman spectra of the dehydrated Sb−V/ZrO_2 series.

ZrO_2 system has dispersed antimony oxide, dispersed vanadium oxide, and the $SbVO_4$ phase. As the Sb−V coverage increases, the formation of $SbVO_4$ is highlighted by new Raman bands close to 452 and 760 cm^{-1} and the decrease in the band of the dispersed vanadium oxide species (1030 cm^{-1}). The excess Sb forms α-Sb_2O_4, with broad Raman bands near 190 and 400 cm^{-1}. Once the formation of $SbVO_4$ has become evident, the transition of the tetragonal to the monoclinic ZrO_2 phase does not occur, in agreement with the trends shown by the XRD pattern of the structural effects of the vanadia phase.

4. Discussion

4.1. Effect of Added Vanadia. *Formation of ZrV_2O_7.* The in situ Raman methodology revealed that vanadia disperses on the zirconia support and that ZrV_2O_7 is formed as the vanadia coverage increases. Its formation takes place more rapidly than that on the ZrOH support. It has been proposed that ZrV_2O_7 develops via interaction of crystalline vanadia with Zr species, which would migrate toward the vanadia crystals.[29] This interpretation does not appear to fit in our work as the formation of ZrV_2O_7 on 8 V/ZrOH at 473 K in the TP-Raman spectra does not uncover the appearance of crystalline vanadia at all (Figure 7A). Figure 5 shows that as the vanadia coverage increases, ZrV_2O_7 forms immediately after or simultaneously with the build-up of crystalline vanadia. The coexistence of V_2O_5 and ZrV_2O_7 at intermediate coverages in both the V/ZrOH and V/ZrO_2 series does not mean that crystalline vanadia is required for the formation of ZrV_2O_7, which appears to form from the dispersed vanadia and amorphous zirconia species. Furthermore, bulk V_2O_5 requires a temperature of 973 K to react with bulk ZrO_2 to form ZrV_2O_7, as shown by Sanati et al.[27] The formation of ZrV_2O_7 at lower temperatures (e.g., 473−673 K) can only be understood in terms of the intimate contact between surface vanadium oxide species and zirconia. In this context, the relevance of the nature of the support (uncalcined ZrOH or precalcined ZrO_2) might provide an indication of the relevance of Zr sites. The V/ZrOH series forms ZrV_2O_7 more readily than the V/ZrO_2 series (4.0 vs 8.0 V atoms/nm^2). This suggests that mobility is very important for the formation of ZrV_2O_7, whereas the presence of crystalline V_2O_5 does not appear to be critical. It should be underlined that Raman spectra in ref 29 show the incipient formation of ZrV_2O_7 at 573 K, before the formation of V_2O_5 during the calcination of vanadia supported on zirconium oxyhydroxide.

Phase Transition. The three crystalline phases of pure zirconia are the monoclinic, which is stable up to 1470 K; the tetragonal, which is stable up to 2170 K; and the cubic, which is stable beyond 2170 K. There is also a metastable tetragonal phase, which is stable below 923 K. The existence of this phase is due to impurities and the effect of crystal size.[30] The presence of vanadium retards the transformation from amorphous to tetragonal zirconia.[15] At calcination temperatures of 673 or 773 K, the transition of the tetragonal to the monoclinic polymorph is retarded by vanadium.[15,29] However, the tetragonal-to-monoclinic transition increases the vanadia coverage at 923 K.[15] These trends are sensitive to whether V and/or Sb have been added to zirconium oxide or oxyhydroxide (series V/ZrO_2 or V/ZrOH). Vanadia induces Zr transformation to the monoclinic polymorph and the formation of ZrV_2O_7 as the vanadia coverage increases. It should be stressed that the transformation to the monoclinic phase also occurs for the V/ZrO_2 series. However, the total transformation into the tetragonal phase requires higher vanadia loadings for the V/ZrO_2 series than for the V/ZrOH series. TP-Raman spectra show that the transformation to the monoclinic phase occurs at lower temperatures for the V/ZrO_2 series than for the V/ZrOH series. This suggests that the formation of the monoclinic polymorph takes place via the tetragonal phase. This would agree with the temperature ranges reported for each phase.[30] Mercera et al. reported that the monoclinic phase increases at the expense of the tetragonal polymorph as temperature increases.[31] Measurements show that the monoclinic phase forms at lower temperatures as the vanadia coverage increases, which further supports the trend reported by Sohn et al., who measured XRD patterns of samples calcined at different temperatures.[15] This trend confirms that the formation of the monoclinic polymorph must occur via the tetragonal phase.

4.2. Effect of Sb Oxide. The lower decrease in the BET area for both the Sb/ZrO_2 and Sb/ZrOH series would be indicative of a very small interaction between the Sb and Zr sites. The addition of antimony to zirconia produces less modification on the support than does the addition of vanadia. At high Sb coverage, the support remains tetragonal. The monoclinic phase observed at low Sb coverage by Raman spectroscopy is not detected by XRD; thus, the domains must be smaller than 4 nm. Furthermore, the precalcined support shows the Sb_2O_3 diffraction pattern, suggesting a weak interaction between antimony and zirconia. The XRD and Raman data show that the presence of the monoclinic phase is most intense for the Sb/ZrO_2 series (Figures 2 and 8). The very low amount of monoclinic phase in the Sb/ZrOH series might arise from the more intimate contact that is expected to occur between Zr hydroxide and Sb than between ZrO_2 and Sb oxide during calcination. The higher sensitivity of the Zr hydroxide precursor than ZrO_2 to an additive has already been reported.[32] Thus, it appears that Sb tends to inhibit the tetragonal-to-monoclinic zirconia phase transition.

4.3. Effect of Sb and V Oxides. In general, zirconia with Sb and V shows a smaller decrease in BET area, a higher stabilization of the tetragonal phase, and the lack of formation of ZrV_2O_7, as shown by the XRD and Raman results. At low Sb−V coverage, vanadia is dispersed on zirconia, and part of the support is monoclinic. It appears that the high dispersion of both Sb and V minimizes the Sb−V interaction, which must limit the capacity of V to promote the transition to monoclinic zirconia. In this sense, the broad Raman bands at 750−950 and close to 452 cm^{-1} would be indicative of the incipient formation of $SbVO_4$.[5] At very low V−Sb coverage, the bands of this compound are weak and coexist with the Raman band of dispersed vanadium oxide species. Thus, vanadia would remain dispersed but would also form compounds with Sb. This would leave part of the vanadium free to promote the ZrO_2 transition to the monoclinic phase. The trends reported above suggest that the ability of V oxide to promote the zirconia transition to the monoclinic phase is stronger than that of Sb oxide to stabilize the tetragonal phase. The scenario is different at high Sb−V coverage, as Sb and V react to form $SbVO_4$, thereby removing the dispersed vanadium species that interact directly with zirconia.

(29) Su, S. C.; Bell, A. T. *J. Phys. Chem. B* **1998**, *102*, 7000.
(30) Yamaguchi, T. *Catal. Today* **1994**, *20*, 199.
(31) Mercera, P. D. L.; van Ommen, J. G.; Doesburg, E. G.; Burggraff, A. J.; Ross, J. R. H. *Appl. Catal A* **1990**, *57*, 127.
(32) Mekhemer, G. A. H.; *Colloids Surf. A* **1998**, *141*, 227.

Sb oxide shows no Raman band at low coverage, like the Sb/ZrO_2 and Sb/ZrOH series. However, according to XRD and Raman data (Figures 3 and 9), at high Sb−V coverage, the Sb that has not reacted with vanadia forms Sb_2O_4, along with $SbVO_4$. The coexistence of these compounds is very attractive for the use of ZrO_2-supported SbV oxides in propane ammoxidation.

4.4. Effect on BET Area. At low vanadia coverage, the BET area of vanadia−zirconia systems prepared on $Zr(OH)_4$ increases, according to Su and Bell[29] and Sohn et al.,[15] after calcination at 773 and 673 K, respectively. Our series, calcined at 923 K, shows a moderate BET decrease at low vanadia coverage and a strong decrease as the vanadia coverage approaches 8.0 V atoms/nm^2. Su and Bell reported a decrease in the BET area as the V coverage approached a full monolayer.[29] However, Sohn et al. did not detect any decrease in the BET values beyond the V monolayer coverage.[15] This might be due to the lower calcination temperature (673 K), where several transformations might not take place, as shown by the TP-Raman spectra obtained in this work and in other studies.[29]

The decrease of the BET areas of the samples is basically related to the crystallization of the support substrate. The full width at half-maximum (fwhm) of the most intense diffraction line of ZrOH at about 30° decreases only slightly for 1.6 V atoms/nm^2 sample but drastically for higher V concentrations. This observation indicates that the increase in crystal size occurs for samples with [V] ≥ 4.0 V atoms/nm^2 in which the BET area dramatically drops. In addition, the fwhm of the same diffraction line remains almost unchanged for the 1.6 Sb atoms/nm^2 sample (cf. Figure 2) whose BET area does not change to a great extent. Both facts indicate that the BET decay is directly related to the development of large ZrO_2 crystals.

In a previous contribution,[33] we observed that ZrOH samples exhibit a type II nitrogen adsorption isotherm with a type H3 hysteresis loop and a very narrow pore size distribution centered at 3.3 nm. Accordingly, incorporation of V and Sb at loading values beyond 1.6 atoms/nm^2 might lead to deposition of the metal oxide precursors in these narrow pores, with subsequent blocking of the support surface accessible to nitrogen molecule. It is also expected that the mobility of the surface species is enhanced upon water removal during the calcination step. Thus, a collapse of the micropore, and perhaps mesopore, network of the original ZrOH sample presumably takes place, with simultaneous development of large ZrO_2 crystals.

ZrV_2O_7 formation (780 and 990 cm^{-1}) might also account for the decrease in the BET area as the vanadia coverage increases because this compound has a very low specific area (Table 1). The fact that the decrease in area is most intense for the V/ZrOH series, which has a more extensive formation of ZrV_2O_7 phase, must be related to collapse of the micropore network of the ZrOH support, followed by solid-state reaction between the outer zirconia layer and surface vanadium species. Another effect of calcination is that the dispersed ZrV_2O_7 phase becomes ordered in tridimensional structures, that can be detected by XRD. The lower decrease in the BET area for both the Sb/ZrO_2 and Sb/ZrOH series would indicate a very small interaction between the Sb and Zr sites. In general, zirconia with Sb and V show a smaller decrease in BET area, a higher stabilization of the tetragonal phase, and absence of the ZrV_2O_7 phase, as shown by the XRD and Raman results.

(33) Larese, C.; Campos-Martin; J. M.; Fierro, J. L. G. *Langmuir* **2000**, *16* (26), 10294.

5. Conclusions

The presence of dispersed vanadium oxide species on ZrO_2 and $Zr(OH)_4$ affects the structure of the zirconia and the BET area after calcination. As the vanadia coverage increases, the transition from the tetragonal to the monoclinic polymorph is more extensive. At high vanadia coverage, the BET area decreases markedly. These trends are stronger for the V/ZrOH series, in which $Zr(OH)_4$ is used as a support. Vanadia coverage also promotes the formation of ZrV_2O_7, which appears to originate from the intimate contact between dispersed vanadium oxide species and the zirconia support. ZrV_2O_7 formation is most evident in the series in which zirconia has not been calcined. These results highlight the formation of ZrV_2O_7 via the intimate contact between V and Zr sites, which might take place at temperatures significantly lower than those required for bulk V_2O_5 and bulk ZrO_2. Antimony tends to stabilize the zirconia phase and the BET area. Vanadia has a strong interaction with the zirconia support, in contrast to Sb oxide. Under the conditions selected in this work, the interaction can occur below a monolayer coverage. Thus, two scenarios might occur when antimony and vanadia coexist on zirconia. There is very little interaction between Sb and V at low Sb−V coverage. Thus, both Sb and V interact directly on ZrO_2, and it appears that the effect of V prevails over that of Sb. At high Sb−V coverage, Sb and V react and form $SbVO_4$, and the excess of Sb is present as Sb_2O_4. Because there is no excess of unreacted surface vanadia, the transition to the monoclinic phase is prevented under the conditions used here.

Acknowledgment. This research was partly supported by the Comisión Interministerial de Ciencia y Tecnología (CICYT), Spain, under Project QUI98-0784, and REPSOL-YPF. CICYT Grant IN96-0053, Spain, funded acquisition of the Raman spectrometer. C.L.P. thanks the Spanish Ministry of Education for a grant to fund his stay in Spain. The authors thank Dr. A. Bahamonde for providing reference zirconia phases.

CM000333V